CHEMICAL 'FINGERPRINTING' AND IDENTIFICATION OF UNKNOWNS IN COUNTERFEIT ARTESUNATE ANTIMALARIAL TABLETS FROM SOUTHEAST ASIA BY LIQUID CHROMATOGRAPHY/TIME-OF-FLIGHT MASS SPECTROMETRY

A Thesis
Presented to
The Academic Faculty

By

Krystyn Alter Hall

In Partial Fulfillment
Of the Requirements for the Degree
Master of Science in Chemistry

Georgia Institute of Technology
December 2005

CHEMICAL 'FINGERPRINTING' AND IDENTIFICATION OF UNKNOWNS IN COUNTERFEIT ARTESUNATE ANTIMALARIAL TABLETS FROM SOUTHEAST ASIA BY LIQUID CHROMATOGRAPHY/TIME-OF-FLIGHT MASS SPECTROMETRY

Approved By:

Facundo M. Fernandez, Advisor
School of Chemistry and Biochemistry
Georgia Institute of Technology

Jiri Janata
School of Chemistry and Biochemistry
Georgia Institute of Technology

Boris Mizaikoff
School of Chemistry and Biochemistry
Georgia Institute of Technology

Date Approved: November 23, 2005

I dedicate this work to my husband, Matthew. Without his constant love and support, it would not have been possible. Matthew, thank you for everything. I love you.

Thank you also to my family and friends who have supported me through my career at Georgia Tech. You all made it what it was.

ACKNOWLEDGEMENTS

I am extremely grateful to my advisor, Facundo Fernandez for his guidance and knowledge throughout this process. Additionally, there were many others who assisted in this work: Paul N Newton, Michael D. Green, David Pizzanelli, Mayfong Mayxay, Arjen Dondorp, Nicholas J White. Additionally, I am grateful to my committee and to all others that assisted me during my time at Georgia Tech.

I am grateful for the funding that was provided by a starter grant from the Society of Analytical Chemists of Pittsburgh to F.M.F. and by startup funds from Georgia Tech Research Corporation. The collection of artesunate samples was funded by the Wellcome Trust of Great Britain as part of the Wellcome Trust-South East Asian Oxford Tropical Medicine Research Collaborations. I am grateful to all who have assisted in the collection of samples.

TABLE OF CONTENTS

LIST OF TABLES

LIST OF FIGURES

LIST OF ABBREVIATIONS

AI……Active Ingredient

CID……..Collision-Induced Dissociation

ESI……..Electrospray Ionization

GC……..Gas Chromatography

HPLC……High-Pressure Liquid Chromatography

KNN……K-Nearest Neighbor

LC……Liquid Chromatography

MS……Mass Spectrometer

S/N……Signal-to-Noise Ratio

TLC……Thin-Layer Chromatography

TOF……Time-of-Flight

u……..unified mass units

WHO……..World Health Organization

SUMMARY

The production and distribution of counterfeit drugs is a serious worldwide health problem. One recent example is the appearance of fake artesunate antimalarial tablets in Southeast Asia. Due to the malevolent circumstances in which these fakes are produced, concern over the presence of toxic tablet ingredients is very much a legitimate health issue. Therefore, quantification of the amount of active ingredient present in tablets marketed as artesunate, a drug used for the treatment of the multidrug-resistant *Plasmodium falciparum* malaria in Southeast Asia required liquid chromatography coupled to mass spectrometry (LC-MS). This quantification allows the classification of the tablets as genuine, sub-therapeutic or fake and the validation of field results using colorimetric tests. During the LC-MS experiments, there were the observations that several of the samples contained a "wrong" active ingredient (AI). This was identified via accurate mass measurements, chromatographic retention time and in-source collision-induced dissociation (CID)as erythromycin, a common antibiotic. Using multivariate unsupervised clustering algorithms, the LC-MS data was utilized for "chemically fingerprinting" the fake tablet samples and investigating the similarities between them. The results of this initial survey show a correlation between

sample origin, the different types of fake authentication holograms found in the packaging and sample composition.

CHAPTER 1

INTRODUCTION

Counterfeit drugs, as defined by The World Health Organization (WHO), are those which are "deliberately and fraudulently mislabeled with respect to identity and/or source".[1] Drug counterfeiting can apply to both branded and generic products and counterfeit medicines may include products with the correct ingredients but with fake packaging, with the wrong ingredients, without active ingredients, or with insufficient active ingredient".[1] Public health is at an increasing risk because of an apparent growing global epidemic of the manufacture and trade of counterfeit pharmaceuticals. For example, over 50,000 people were inoculated with fake meningitis vaccines in 1995 in Nigeria, possibly resulting in the deaths of 2,500 children.[1] In Haiti, Nigeria and Bangladesh approximately 400 children have died after ingesting counterfeit paracetamol (acetaminophen) syrup that was made using ethylene glycol, a toxic industrial solvent.[2-4] Because of multiple fake drugs, an estimated 192,000 people died in the People's Republic of China in 2001.[5] It is believed that approximately 10% of all pharmaceutical products sold worldwide are counterfeits[2,6], representing a $32 billion/year industry. However, only a minority of counterfeit drug incidents are reported to the appropriate enforcement agencies, and thus numbers of those affected

by counterfeit drugs are likely to be grossly underestimated.[7, 8] It has been estimated that more than half of counterfeit drugs available worldwide contain no active ingredients or contain a different active ingredient than that stated on the labeling and that nearly 10% contain contaminants.[8]

Since the late 1990s, counterfeit drugs that mimic drugs used for the treatment of potentially-fatal tropical diseases, such as malaria, have been detected in increasing numbers. Malaria is a major health problem in many tropical countries, specifically in sub-Saharan Africa and Southeast Asia.[9] Each year, between 300 and 500 million people in Asia and Africa contract *Plasmodium falciparum* malaria and 1.5 million people, mostly children, die.[10] Until an effective vaccine is found,[11, 12] the control of malaria still depends on the use of effective antimalarial drugs and bednets. However, during the past three decades malaria control has been hampered by an increase in the prevalence of drug-resistant malaria parasites.[11, 13] This is a particularly severe problem in SE Asia, where reduced sensitivity to other antimalarials such as chloroquine, sulphadoxine-pyrimethamine, halofantrine, mefloquine and quinine has been reported.[14]

Artesunate, an artemisinin derivative (Figure 1), is now the recommended treatment in many countries where drug-resistant malaria parasites exist[9] and has become the target of an extremely sophisticated and prolific counterfeit drug trade.[7] This includes the counterfeiting of both the

artesunate tablets and packaging, which, to the untrained eye, look extremely similar to the authentic product.[7, 15, 16] Counterfeit artesunate tablets are commonly found at shops and pharmacies in mainland

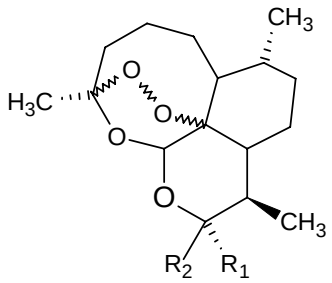

R_1, R_2=O	Artemisinin
R_1=H, R_2=OH	Dihydroartemisinin
R_1=H, R_2=OCH_3	Artemether
R_1=H, R_2=OCH_2CH_3	Arteether
R_1=H, R_2=$OCH_2C_6H_5CO_2H$	Artelinic Acid
R_1=H, R_2=$OCOCH_2CH_2CO_2H$	Artesunic Acid

Figure 1: Structures of artemisinin and its derivatives.

Southeast Asia[17] where they have probably resulted in the deaths of numerous patients who would have otherwise survived the malarial infection.[18] In addition, counterfeit quinine and mefloquine tablets and artemether injections have been found in Asia.[15] In a study conducted in 1999-2000, 38% of all artesunate tablet blisterpacks bought in Cambodia, Laos, Burma, the Thailand/Burma border, and Vietnam contained no active ingredient. [17,19] In a subsequent follow-up study conducted in the same area, in 2001-2, 53% of artesunate blisterpacks were counterfeit, suggesting that the problem may be worsening.[19]

CHAPTER 2

LITERATURE REVIEW

The chemical analysis of counterfeit drugs poses a challenging task in terms of sample throughput, dynamic range and identification of unknowns. Recently, Deisingh has reviewed the analytical methods used to investigate counterfeit drugs.[20] These methods include Raman spectroscopy[21], near infrared spectroscopy[22-24], thin layer chromatography (TLC) [25], gas chromatography (GC)[20], liquid chromatography (LC)[26] and LC coupled to tandem MS (LC-MS/MS)[6].

In the particular case of the chemical analysis of counterfeit antimalarial samples, only colorimetric and bulk property tests have been used thus far.[27] Green et al. have developed a colorimetric test based on the Fast Red TR dye[28, 29] for detecting artemisinin derived compounds such as artemether, artesunate and dihydroartemisinin in tablets. This colorimetric method was used in the first two field studies to investigate the prevalence of counterfeit artesunate.[17] During these studies the usefulness of visual 'taxonomic' cues in detecting counterfeit artesunate was also demonstrated: an observer, who was unaware of the colorimetric test results, examined the holograms, bar codes, printing, crimping, color, size, weight, consistency, and taste of the putative artesunate tablets and then classified them as genuine or fake.[17] Visual

inspection of the tablets was in exact agreement with the colorimetric test only in the first survey[17], but not in the second.[19] The counterfeiters appear to have responded to this information by producing more sophisticated counterfeit holograms and packaging, making it very difficult to distinguish the counterfeit and genuine drugs.[30, 31]

The objectives of this work were two-fold. The first objective was to develop an LC-MS methodology suitable for evaluating the artesunate contents of a set of genuine and fake artesunate tablets collected in SE Asia and to validate the results obtained in the field by the rapid artesunate colorimetric test. The second objective was to "chemically fingerprint" the confirmed fake artesunate samples in order to examine, via multivariate clustering techniques, the similarities and differences between them. Even in the absence of the expected active ingredient, the abundance, molecular weight distribution and chromatographic retention time of the excipients and impurities present in counterfeit drugs constitutes a unique chemical fingerprint.[32] To date, this seems to be one of the first reported attempts to systematically study the composition of a set of counterfeit drug samples collected over a vast geographical area. The methodology presented here should prove useful in investigating other cases of drug counterfeiting.

CHAPTER 3

EXPERIMENTAL

3.1 Standards and Solvents

Artesunate (CAS # 88495-63-0) and erythromycin, (CAS # 114-07-8) were obtained from Apin Chemicals Ltd and Fluka Biochemica, respectively, and used without further purification. Artesunate standards were prepared in HPLC grade methanol (Sigma Aldrich, St. Louis, MO). Erythromycin standards were prepared in a 50/50 solution (v/v) of HPLC grade acetonitrile (Sigma Aldrich, St. Louis, MO) and pure water (Barnstead International, Dubuque, IA). All standards and samples were filtered through a 0.45µm PTFE membrane filter (Pall Corporation, Ann Arbor, MI) before analysis. Fresh standards were prepared on a daily basis from stock solutions that were stored at 4° C.

3.2 Sample Collection and Preparation

Counterfeit and genuine artesunate tablets were collected in a wide area of SE Asia encompassing the following countries: Laos, Burma (Myanmar), Vietnam, Cambodia, Hong Kong and Thailand.[17, 23, 29] Prior to analysis, tablets were crushed with a mortar and pestle and thoroughly homogenized. For artesunate quantification, approximately 5 mg of sample were suspended in 1 mL of methanol and extracted for 2 hours on

a rotary shaker. For erythromycin quantification and tablet "fingerprinting," approximately 100 mg of sample were suspended in 10 mL of a 50/50 acetonitrile/water (v/v) mixture and extracted on a rotary shaker for 2 hours. Following extraction, all samples were filtered through a 0.45µm PTFE membrane filter. Tablet extracts were kept refrigerated (4° C) until analysis. Prior to analysis, samples were diluted with methanol or 50/50 acetonitrile/water (v/v) on a case-by-case basis.

3.3 Liquid Chromatography –Mass Spectrometry for Tablet "Chemical Fingerprinting"

LC was performed on an Agilent 1100 system equipped with a solvent degasser, a binary pump, a thermostated column compartment (held at 25ºC), an autosampler and a diode array detector. A 2.1mm ID, 150mm long Zorbax Extend-C18 column (Agilent, Palo Alto, CA) equipped with a precolumn was used in all of the experiments. The LC was operated at a flow rate of 200 µL min^{-1}, with an injection volume of 20 µL. The binary pump used HPLC grade water with 0.01% acetonitrile as mobile phase A and acetonitrile as mobile phase B. The LC gradient started at 5% B and ramped to 45% B until 7 minutes, then increased to 100% B from 7 to 8 minutes and held at 100% B until 12 minutes. The system was set with a 4 minute post-run time to equilibrate the column to the original mobile phase composition. To ensure maximum reproducibility, all the organic extracts obtained from fake tablets where run on the same day and by

triplicate sequential injections and blank runs were inserted between sample runs to eliminate sample carryover.

The Agilent 1100 LC system was coupled to an AccuTOF orthogonal extraction TOF MS (JEOL, Peabody, MA) via an orthogonal electrospray interface operating at 2kV. Although in principle, negative-ion electrospray ionization would be the first choice for artesunate (due to its carboxylic side chain, Figure 1) positive-ion mode electrospray was used to ensure that other active ingredients not containing phenolic or carboxylic moieties (if present) could be simultaneously detected. The mass spectrometer electrospray source ion optics settings were as follows: inlet orifice, 30 V; ring electrode, 8 V, first skimmer, 5 V; ion guide bias voltage, 26 V; ion guide RF amplitude, 2000 V. The nebulizing gas flow rate, the desolvation gas flow rate, the needle chamber compartment temperature and the inlet orifice temperature were: 1.0 L min^{-1}, 2.5 L min^{-1}, 250ºC and 80ºC, respectively. The multi-channel plate detector was set to 2500 V. Data collection was performed with a FastFlight digital signal averager (ORTEC, Oak Ridge, TN) with a data sampling interval of 0.5 nsec and a spectrum recording interval of 0.4 sec. Accurate mass measurements were performed using a 1 µM solution of reserpine for mass drift compensation. The average mass resolution observed was between 6000 and 6800 (FWHM). The NIST mass spectral library (version 2.0 a) and

SciFinder scholar (CAS, 2004) were used to search for unknown compounds.

3.4 Active Ingredient Quantification

All samples were analyzed in a blind fashion (i.e. without *a priori* knowledge of the results of the colorimetric test or the sample origin) to avoid any possible bias. Artesunate was quantified using similar LC-MS settings as previously described but with the following differences: HPLC grade water with 0.01% methanol was used as phase A and methanol as mobile phase B. The LC solvent gradient started at 35% B for 3 minutes. From 3 minutes and until 18 minutes it was ramped to 100% B, where it was held until 30 minutes. After this, it was ramped back down to 35% B using a 15-minute ramp. The system was set with a 7.5 minute post-run time to equilibrate the column prior to the next run. With this gradient, the retention time for artesunate was 18.1 ±0.4 min. The settings of the TOF mass spectrometer ion source optics were as follows: inlet orifice, 20 V; ring electrode, 10 V, second skimmer, 2 V; ion guide bias voltage, 36 V; ion guide RF amplitude, 2000 V.

Erythromycin was quantified using flow injection-MS. A Vici Cheminert M6-liquid handling pump (Valco Instruments Co. Inc. Houston, TX) operated at 200 µL min^{-1} was connected to a manual 6-way HPLC injection valve equipped with a 20 µL loop (Valco). The mobile phase

consisted of 50% acetonitrile in water. The calibration curve for erythromycin was linear between 2 nM and 145 nM. Mass selected chromatograms allowed the creation of external calibration curves for quantification purposes. The area of the mass-selected chromatographic peaks was integrated using MassCenter software v.1.0 (JEOL).

3.5 Data Processing and Analysis for Chemical Fingerprinting

Time-resolved mass spectral data was exported from the AccuTOF instrument in JEOL-DX ASCII format using a custom-made chromatographic peak processing list. Conventional peak processing lists only allow spectra corresponding to chromatographic retention times where peaks are detected to be exported. However, our multivariate clustering approach requires every LC-MS run to be exported as an intensity matrix consisting of a fixed number of rows (retention times) by a fixed number of columns (m/z values). In order to export mass spectra at *every* retention time an artificial train of sample injection pulses (and thus detectable "chromatographic" peaks) was generated by intermittently pumping a 5 µM reserpine solution with the Vici Cheminert M6 pump. This pump was software-controlled by a timing routine which alternated between 20 µL injections at a flow rate of 200 µL min^{-1} followed by a 10 s pause. In this way, the MassCenter 'spectrum processing wizard' was forced to generate an entry in the chromatographic peak processing list

at repetitive times. This processing list allowed the exportation of LC-MS data of fake artesunate tablets which resulted in 44 mass spectra, each averaged over a 16.36 s retention time interval.

Triplicate runs of twenty three fake artesunate tablets were processed using Matlab v. 7.0 (The MathWorks, Natick, MA). The routines included in the PLS Toolbox (Eigenvector Research, Inc., Manson, VA) were used for multivariate clustering. All calculations were performed on a dual-processor Dell Optiplex PC with 1GB RAM (Dell, Round Rock, TX). The parameters for the construction of the matrices used for multivariate clustering in Matlab as follows: first was the creation of a 44 by 18,001-element matrix for each sample run filled with zeroes. Then, this matrix was filled with the LC-MS intensity values obtained from the JEOL ASCII files, which were rounded to the nearest 0.1 u. These intensity matrices contain 44 averaged chromatographic retention times and 18000 m/z values (from 200 to 2000 u every 0.1 u). After the creation of the intensity matrices, the data for the triplicate runs for each sample was visually inspected to eliminate any possible outliers (none found) and then averaged into a single matrix per sample. The m/z values between 200-340 u and 1200-2000 u for these averaged matrices were set to zero as they did not contain any significant information. In order to further remove noisy variables, a signal threshold was applied to all the matrices by setting to zero any other matrix element whose intensity was lower than

1200 arbitrary units. Average matrices were unfolded into a 44x18,001=792,044 element vector which contained, in one row, all mass spectra ordered by increasing retention times. The vectors of all 23 samples were then combined into a single 23 by 792,044 matrix. Multivariate clustering was performed on this matrix using K-nearest neighbor (KNN) hierarchical clustering.[33]

CHAPTER 4

RESULTS

4.1 Artesunate Content of Antimalarial Drugs from SE Asia

Prior to quantification by LC-MS, the electrospray response of standard artesunate solutions was characterized. Artesunate yielded complex positive-ion electrospray spectra even at low capillary-skimmer potential differences and low concentrations. A representative electrospray spectrum of artesunate is shown in Figure 2. Multiple adducts and fragments are observed. The major adduct ions present were $[M+NH_4]^+$ (m/z=402), $[M+Na]^+$ (m/z=407), $[2M+NH_4]^+$ (m/z=786), and $[2M+Na]^+$ (m/z=791). The $[M+H]^+$ ion was not observed, regardless of the organic solvent used to prepare the standards. The total ion intensity of the Na^+ and NH_4^+ adduct ions decreased when more energetic desolvation conditions were used. For a 4 µM artesunate standard, the relative abundance of the $[M+Na]^+$ adduct decreased by a factor of 103 and the $[M+NH_4]^+$ adduct ion disappeared when the capillary-skimmer potential difference was increased from 20 V to 80 V. Increased stability of the Na-adducts has also been observed for other drug compounds such as corticosteroids.[34] The extent of dimer formation was also dependent on the skimmer-capillary voltage. Upon an increase in capillary-skimmer potential difference from 20 V to 80 V, the dimer was

completely dissociated; increasing the abundance of the monomeric adducts and fragments. Fragment ions were observed at declustering

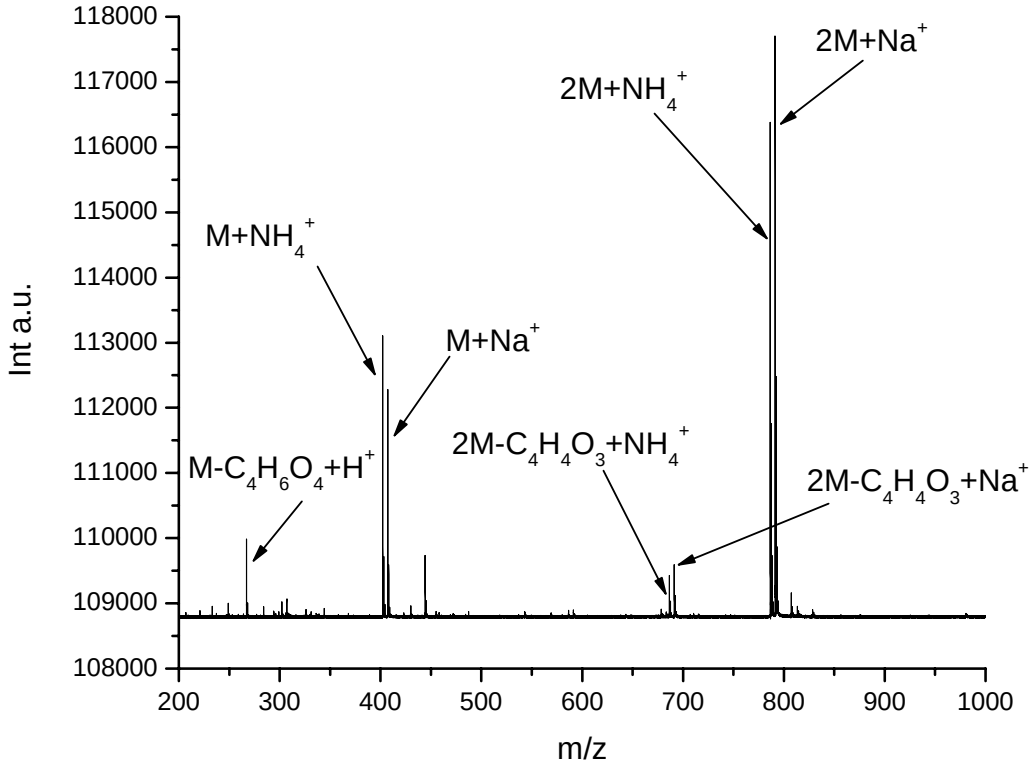

Figure 2: Typical positive ESI spectra of 4 μM artesunate solution in a 50:50 MeOH:water mixture infused at 200 μl min^{-1} (1 minute acquisition). The capillary-skimmer voltage difference was 20Vand the electrospray needle voltage was 2000V.

potential differences as low as 20 V (the minimum declustering potential needed to effectively transmit ions). The most abundant in-source CID fragment ions observed were produced by the loss of $C_4H_6O_4$ (m/z=118)

from the $[M+H]^+$ ion ($[M-C_4H_6O_4+H]^+$, m/z=267) which may explain the absence of the protonated adduct in the spectrum. Dimer ions produced the $[2M-C_4H_4O_3+Na]^+$ and $[2M-C_4H_4O_3+NH_4]^+$ fragments. At capillary-skimmer potential differences of 80V or higher, other ions such as the $[M-HCOOH+Na]^+$ fragment were also observed.

After the positive electrospray response was characterized mass-selected LC-MS chromatograms for artesunate standards at varying m/z window widths were obtained in order to maximize sensitivity and minimize interferences during artesunate determination. To select the optimum m/z window, the signal-to-noise ratio (S/N) at varying window widths (m/z) for two different adduct ions were examined (Figure 3). As it can be seen in Figure 3 window widths lower than 0.06 for $[M+Na]^+$ and 0.1 u for $[M+NH_4]^+$ resulted in a decrease in the observed S/N due to the exclusion of a significant fraction of the mass spectral peak intensity in the mass selected chromatogram. Both for $[M+Na]^+$ and $[M+NH_4]^+$, S/N was maximum at a window width of 0.2 u after which it remained constant or even decreased due to the inclusion of noise. A window width of 0.2 u was therefore used for all LC-MS artesunate quantification experiments.

Dimer formation reduced the linear working range of the calibration curves. At artesunate concentrations higher than 9 µM, the slope for the $[M+Na]^+$ and $[M+NH_4]^+$ calibration curves was no longer constant and a significant increase in the dimer signal intensity was observed. Ortelli et al.

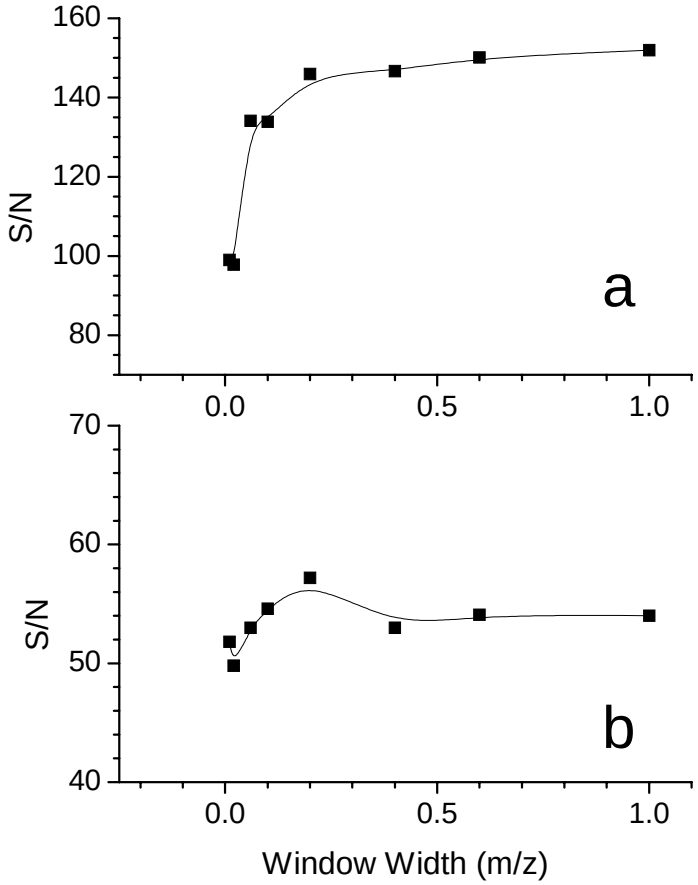

Figure 3: Signal to noise ratio for the artesunate chromatographic signal versus window width used in the generation of selected mass chromatograms. (A) [M+Na]+ signal of a 1.1 µM solution, (B) [M+NH4]+ signal of a 2.1 µM artesunate solution. Signal-to-noise ratios were determined using a built-in function in the MassCenter software v.1.0.

have observed a similar behavior for different artemisinins and demonstrated that the addition of ion-pairing alkylamines to the LC mobile phase dramatically reduces multimer formation and increases the dynamic linear range.[35] We chose not to use such an additive, to prevent formation of ion pairs with unknown compounds which could complicate

the early detection of unexpected active ingredients. Fleckenstein et al. have recently reported the use of the $[M-C_5H_8O_6+H]^+$ fragment (m/z=221 u) for quantification of artesunate in human plasma.[36] However, that particular fragment ion was not observed in our experiments, regardless of the declustering voltage used. In an attempt to increase the dynamic linear range and accommodate the wide range of artesunate concentrations found in our sample set, we investigated the use of the high-energy $[M-HCOOH+Na]^+$ fragment ion for quantification purposes. However, we found that for this ion, the repeatability of triplicate injections of artesunate standards could be as poor as 25 % (RSD), whereas for the ammonium and sodium adducts it ranged from 2% to 8%. Therefore, both the Na^+ and NH_4^+ ion adducts were used for quantitation purposes.

Table 1 shows the artesunate content in selected tablets collected in Vietnam, Myanmar (Burma), Laos and Cambodia. This sample subset represents only those tablets in which artesunate was positively detected via colorimetric methods. The expected amount of artesunate in these tablets is 50 mg/tablet. The amount of artesunate in most of the collected tablets falls within a ±15% range of the expected value, thus validating the results of the artesunate colorimetric test. Interestingly, one tablet collected in Siem Reap (Cambodia) showed an amount of artesunate (20 mg/tablet) substantially lower than the accepted range, and thus it should be considered substandard. Substandard artesunate tablets pose

Table 1: Sample origin for a set of artesunate tablets which tested positive in field colorimetric tests. The concentration of artesunate was obtained as the average from two separate determinations based on the $[M+NH_4]^+$ ion signal at m/z=402 and the $[M+Na]^+$ ion signal at m/z=407. The expected artesunate content is 50 mg/tablet.

Sample Code	Sample origin/ collection place	Colorimetric Test Result	Artesunate Content (mg/tablet) via LC-MS
5	Mae La, Thai/Myanmar border	+	54 ± 1
18	Ho Chi Minh City, Vietnam	+	51 ± 6
31	Vietnam	+	54 ± 5
32	Mueang Feuang, Laos	+	49 ± 6
39	Myitkyina, Myanmar	+	42 ± 12
12064	Sekong, Laos	+	62 ± 4
12065	Sekong, Laos	+	57 ± 3
12068	Attepeu, Laos	+	65 ± 14
13008	Siem Reap, Cambodia	+	21 ± 2
13013	Ko Kong, Cambodia	+	58 ± 3
63001	Phnom Phenh, Cambodia	+	56 ± 2
10401/1	Pakse, Laos	+	57 ± 4
10401/2	Pakse, Laos	+	50 ± 7

a great danger to public health because they can create an environment that selects drug-resistant parasite strains.[37] The colorimetric artesunate test is unable to distinguish between standard and substandard tablets, emphasizing the need for quantitative (or at least semi-quantitative) analysis methods. Table 2 shows the artesunate quantitation results for tablets that tested negative by the Fast Red dye test. Although all of these samples were labeled as being manufactured by Guilin Pharma (Guilin, Guangxi, People's Republic of China) and had seemingly authentic holograms on their packaging, they did not contain

artesunate in detectable amounts (less than 1 µg). Overall, 64 % of all the artesunate samples did not contain the expected active ingredient, confirming previous findings by Rozendaal[18], Newton et al. [17, 31] and Dondorp et al.[19] and the most recent findings by de Veij et al.[38] which indicated the widespread distribution of these fakes in mainland SE Asia.

4.2 Identification of the "Wrong" Active Ingredients

During artesunate quantitation, it was noted that several fake artesunate tablets described in Table 2 showed intense chromatographic signals with m/z values that could not be assigned to any artesunate adducts or fragments. Samples 12050, 12052, 12053, 12054, 12057, 12060, 12061 and 12062 (see Table 2), presented similar peaks in the 700-750 m/z range, but with different intensities. This finding suggested that unexpected active ingredients were present in these fake artesunate samples. The presence of wrong AIs in counterfeit antimalarials is not uncommon. Some of the early counterfeit artesunate (collected in or before 1999) contained chloroquine which may have been added to give the counterfeits a bitter taste, as there is a tradition in SE Asia that antimalarials should be bitter.[39] However, chloroquine has very low antimalarial efficacy throughout mainland SE Asia.

Table 2: Sample origin and type of fake holograms found in a set of artesunate tablets which tested negative in field colorimetric tests. The classification of the fake holograms is detailed in the text. N/D=not detected.

Sample Code	Sample origin/ collection place	Fake Hologram Type	Colorimetric Test Result	Artesunate Content (LC-MS)
13	Myitkyina, Myanmar	1	-	N/D
980201	Ho Chi Minh City, Vietnam	1	-	N/D
29	Ho Chi Minh City, Vietnam	2	-	N/D
97	Ho Chi Minh City, Vietnam	2	-	N/D
12050	Pakse, Laos	8	-	N/D
12051	Pakse, Laos	3	-	N/D
12052	Pakse, Laos	12	-	N/D
12053	Pakse, Laos	13	-	N/D
12054	Pakse, Laos	5	-	N/D
12055	Pakse, Laos	3	-	N/D
12056	Pakse, Laos	4	-	N/D
12057	Pakse, Laos	8	-	N/D
12058	Pakse, Laos	8	-	N/D
12060	Salavan Laos	8	-	N/D
12061	Salavan Laos	5	-	N/D
12062	Salavan Laos	12	-	N/D
12063	Salavan Laos	3	-	N/D
12067	Attepeu, Laos	3	-	N/D
12070	Paksong, Laos	4	-	N/D
12071	Paksong, Laos	3	-	N/D
13007	Siem Reap, Cambodia	Yet to be classified	-	N/D
13011/1	Anlong Veng, Cambodia	3	-	N/D
13011/2	Anlong Veng, Cambodia	3	-	N/D

Sample 12053 was chosen to further investigate the most prominent spectral peak in the 700-750 u region because of its lower intensity which made it more prone to accurate mass measurements. The monoisotopic measured mass of the most intense peak was 734.4 u. In a first approach, we assumed that this signal corresponded to the $[M+H]^+$ adduct ion.

Accurate mass analysis was then performed on sample 12053 extract using reserpine (m/z=609.2812 u) for mass scale drift correction purposes, yielding an exact mass value of 734.4703 u. The closest match (-0.20 ppm) to this value was found for an elemental composition of $C_{38}H_{64}N_5O_9$. However, an electronic search revealed no common pharmaceuticals with this composition. The following candidate elemental composition was $C_{37}H_{68}NO_{13}$ with a mass difference of 1.62 ppm and a theoretical mass equal to 734.4691 u. A search within the NIST mass spectral database of this composition returned two matches, only one being an easily-obtained chemical compound. This compound was the common antibiotic erythromycin.

Because of the severity of this finding, further confirmation of our accurate mass results was obtained by additional experiments. Figure 4 shows total ion chromatograms for both an erythromycin standard and sample 12053 showing matching retention times of 13.38 and 13.54 minutes, respectively. Figure 5 shows accurate-mass in-source CID spectra of both the standard and sample obtained in LC-MS function switching mode. The most intense fragment at m/z=576 observed for the erythromycin standard corresponds to the ion with elemental composition of $C_{29}H_{54}NO_{10}$ due to the loss of the cladinose sugar[40] ($C_8H_{14}NO_3$, m/z=158). A similar fragment ion was observed for sample 12053. The relative abundance of the $[M+H]^+$ isotopic peaks was also examined

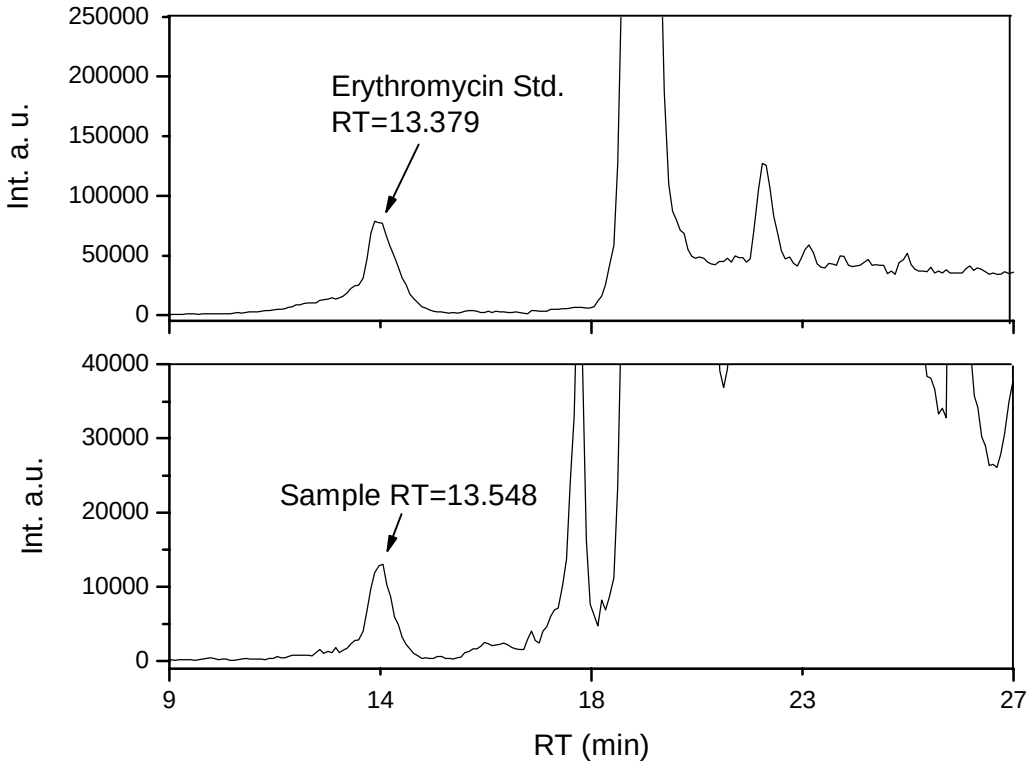

Figure 4: Total ion chromatogram for an erythromycin standard (top) and sample 12053 (bottom). The peak at retention time (RT) =13 minutes corresponds to the $[M+H]^+$ erythromycin ion. The signals observed after 18 minutes correspond to the sum of intensities of solvent cluster ions and solvent impurities. See Experimental for LC gradient settings.

which, were100/40.6/13.2/3.1 for sample 12053 and 100/41.7/11.1/2.2 for the standard, further confirming our finding. Follow-up experiments demonstrated that out of the twenty three tablets containing no artesunate (Table 2), nine tablets contained erythromycin.

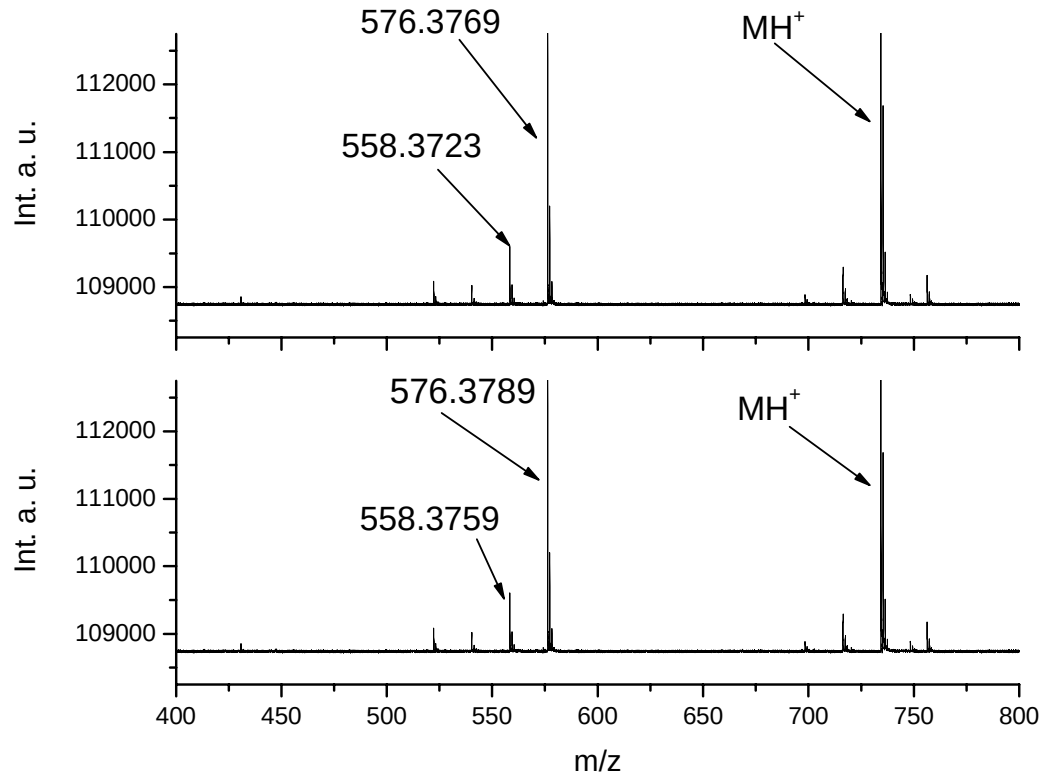

Figure 5: Accurate-mass electrospray in-source CID spectra of erythromycin standard (top) and sample 12053 (bottom). Capillary-skimmer voltage difference was 60V. The peaks at m/z 576 and m/z=558 correspond to the $C_{29}H_{52}NO_9$ and $C_{29}H_{54}NO_{10}$, fragment ions.

4.3 Characteristics of the Packaging of Fake Artesunate Tablets

To this date, we have found at least thirteen different types of counterfeit artesunate tablet samples, based on the packaging appearance and holograms.[17, 19, 31, 41] In this survey, we included samples belonging to most of these types. It is outside of the scope of this article to describe in detail each type of fake hologram that we have found so far, and only a brief description is given here and in Appendix A.

The genuine artesunate hologram from Guilin Pharma (Figure 6A) is a 14 mm diameter self-adhesive label made in the People's Republic of China. This hologram was developed by Guilin Pharma as a security device in response to the first type (Type 1, see Table 2) of counterfeit artesunate that circulated without a hologram attached.[41] The most interesting feature of the genuine hologram is that the outer ring is comprised of small grating segments (see Figure S-1). The "Type 2" fake hologram (Figure 6B) affixed to counterfeit artesunate is made from diffractive "rainbow" foil, commonly used on counterfeit products, and is not a hologram; just a sticker (see Appendix: Figure S-2 for more details). As diffractive rainbow foil is widely sold as a decorative material, it is relatively simple to use this foil for manufacturing copies of the genuine holograms. Fake hologram Types 8, 12 and 13 (Table 2) are foil stickers similar to Type 2, but Type 8 and 12 have a different mountain outlines and Type 13 is a sticker without any discernable pattern. Type 5 is also a sticker in which the mountain outline, waves and circular surrounds are comprised of thousands of small dots. The Type 3 fake holograms (Figure 6C) attached to counterfeit "artesunate" is a simple 2D origination where the image is comprised of two exposures of diffractive color, one of which is much brighter than the other (Figure S-3). The Type 4 fake hologram (Figure 6D) is very similar in appearance to the genuine hologram, despite

being manufactured using different techniques. In this case, the hologram is comprised by a clean, 2D image in two contrasting colors, much brighter than the genuine hologram (Figure S-4).

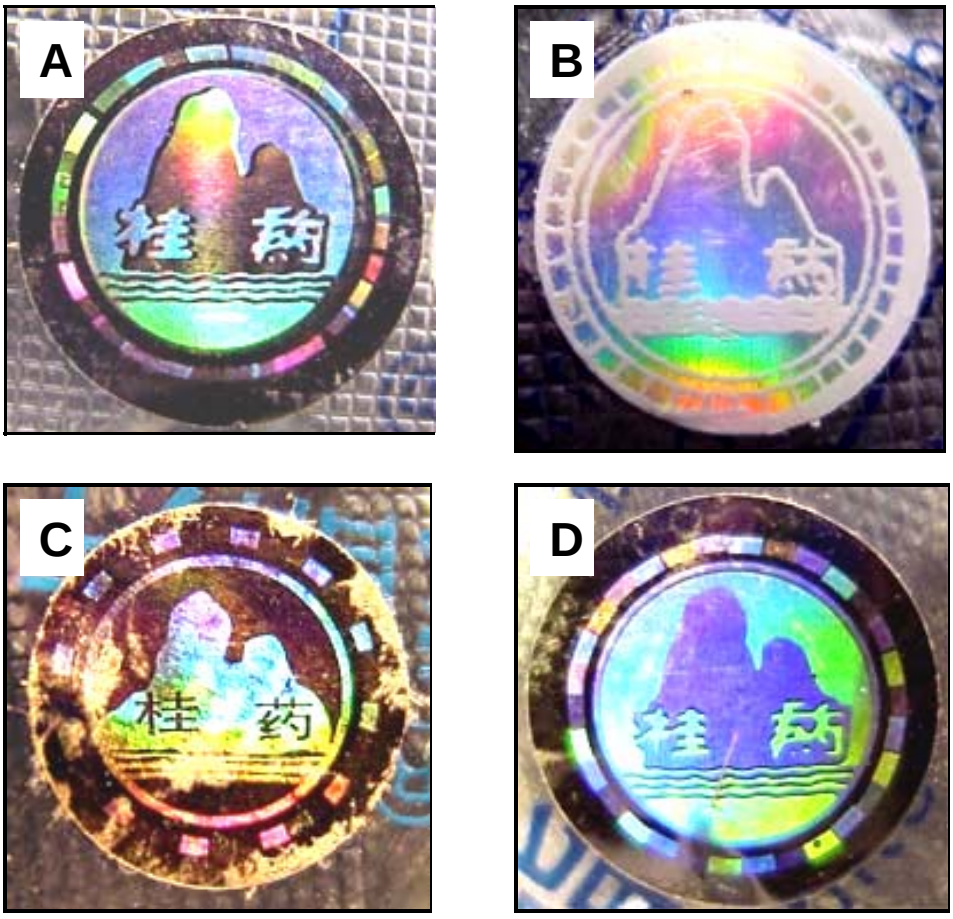

Figure 6: Genuine and fake holograms present in the artesunate tablets packaging. (A) Genuine artesunate hologram (Guilin Pharmaceuticals), (B) Type 2 fake hologram, (C) Type 3 fake hologram, (D) Type 4 fake hologram.

4.4 Multivariate Clustering of LC-MS Chemical Fingerprints

In order to investigate the correlation between a samples origin, the presence of wrong active ingredients and the type of fake holograms observed in the packaging, multivariate clustering was performed on the LC-MS intensity matrices. First, the data in these matrices were visually inspected. Figure 7 shows contour plots for all averaged intensity matrices obtained for the fake artesunate tablets included in this study. Several similarities between samples can be readily found by visual inspection. Samples 12050, 12052, 12054, 12057, 12060, 12061 and 12062 show similar fingerprints; all eight of them are characterized by two distinct features. First, these samples present a polymeric species eluting at 2.1 min, characterized by peaks with a 171 u spacing. The second common characteristic of these samples is, as mentioned before, the presence of erythromycin. When these samples were analyzed via Raman spectroscopy, it was determined that these samples also contain calcite ($CaCO_3$) and that several of them, samples 12060, 12061, and 12062 also contain paracetamol.[38]

Samples 980201 and 29 from Vietnam and 13007 from Cambodia, present fairly uninformative chemical signatures which could be considered compatible with the absence of any active ingredients and/ or the presence of inorganic excipients not extracted during the sample preparation step. One of the most common inorganic diluents for tablet

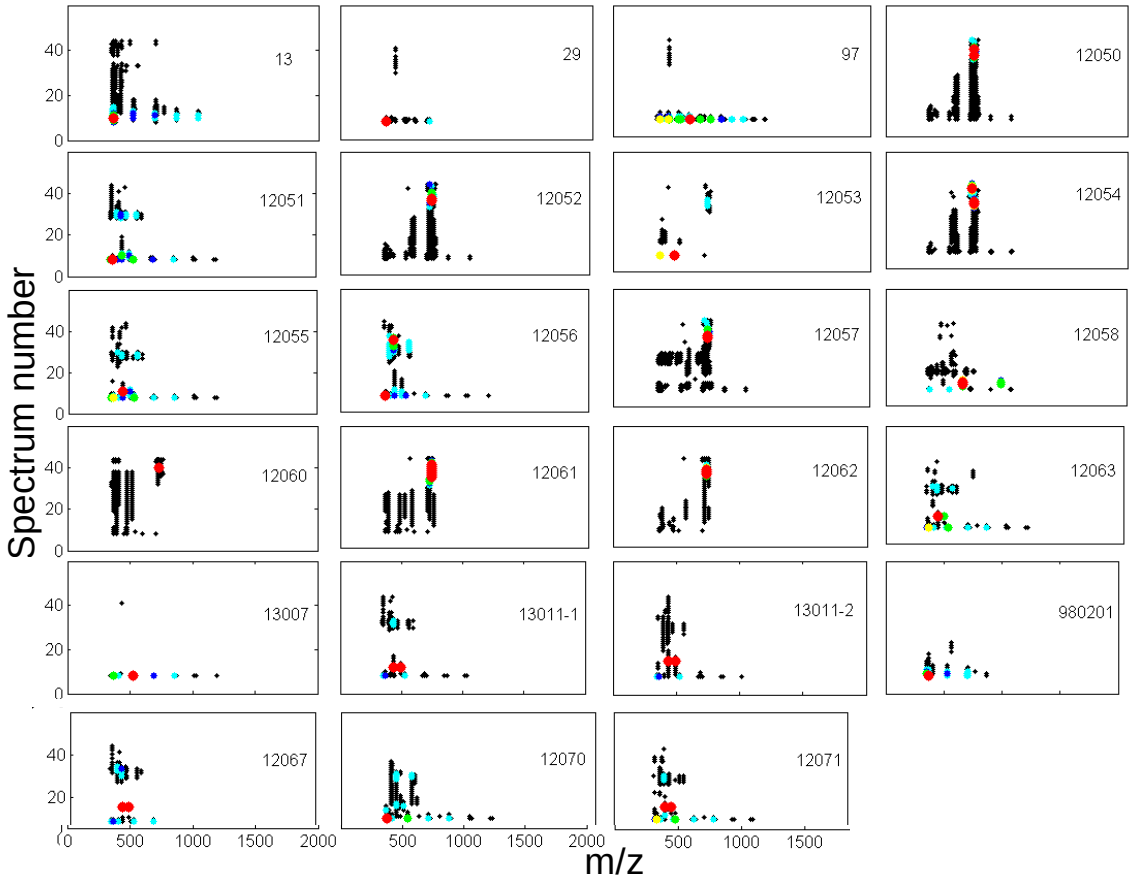

Figure 7: Chemical fingerprint plots of fake artesunate tablets. Sample code is indicated above each plot. Each tablet's data is the average of three LC-MS runs. The x-axis represents m/z values and the y-axis represents the spectrum number collected at increasing chromatographic retention times. These plots are a bidimensional representation of an LC-MS intensity matrix with MS mass-to-charge values as columns, and spectrum number as rows. Larger red dots denote the most intense signals whereas black small dots represent the weakest ones. Signals with intermediate intensity were coded according to the following color scale: yellow>green>cyan>blue.

formulations is $CaCO_3$.[42] Indeed, when dilute acid was added to these samples, effervescence was observed. The presence of $CaCO_3$ was also validated via Raman spectroscopy.[38]

The signal pattern observed in the chemical signatures for samples 13011/1 and 13011/2 from Along Veng in Cambodia are very similar. These tablets come from two different, but physically identical blister packs, bought at the same time from the same shop. The lack of refrigerated storage of the samples in shops and pharmacies in the seasonally high ambient temperatures in SE Asia (up to 40^0C) may be the cause of the small differences between the samples' fingerprints. These samples show a similar polymeric peak eluting at 2 min, with a 162 u spacing, consistent with small monomeric units of hexose, probably derived from partially-extracted low molecular starch-derived compounds (starch is a common filler for pharmaceutical tablets).[42]

Following visual inspection of the data, unsupervised multivariate pattern recognition was performed on the LC-MS intensity matrices as described in Chapter 3.5. Figure 8a presents the KNN dendrogram for the unfolded LC-MS data of counterfeit artesunate tablets extracts. The first salient feature of this figure is that samples 12054, 12061, 12057, 12052, 12050, 12062, and 12060, are clustered towards the top portion of the, dendrogram in a nested fashion. All these samples were collected in Laos and presented intense erythromycin signals and rainbow foil stickers(not

fake holograms). Closer inspection of this sample subset (see for example sample 12052 in Figure 9) revealed several additional peaks in the erythromycin region. Accurate mass measurements were performed on all these peaks, and the following chemical compounds were identified: erythromycin B (theoretical m/z=718.4714 u, observed m/z=718.4742 u); erythromycin C (theoretical m/z=720.4534 u, observed m/z=720.4547); erythromycin E (theoretical m/z=748.4483 u, observed m/z=748.4503 u); erythromycin F (theoretical m/z=750.4640 u, observed m/z=750.4633 u), and anhydroerythromycin (theoretical m/z=716.4585 u, observed m/z=716.4576 u). Only erythromycin A was detected in sample 12053. Erythromycin formulations generally contain more than one type of erythromycin, with erythromycin A being the most abundant and generally referred to only as erythromycin.[43] To further explain the clustering of the erythromycin-containing samples in the KNN dendrogram, we quantified erythromycin A via flow injection MS (Table 3). Fake "artesunate" tablets contained a total amount of erythromycins that ranged from 20 to 190 mg/tablet and thus, these samples could have significant therapeutic activity for sensitive bacterial infections, but no activity in malaria infections. The order of the erythromycin-containing samples in the dendogram followed their erythromycin content, except for sample 12054, which was placed at the top of this diagram and contained 27 mg erythromycin-A/g tablet. This indicates that the absolute

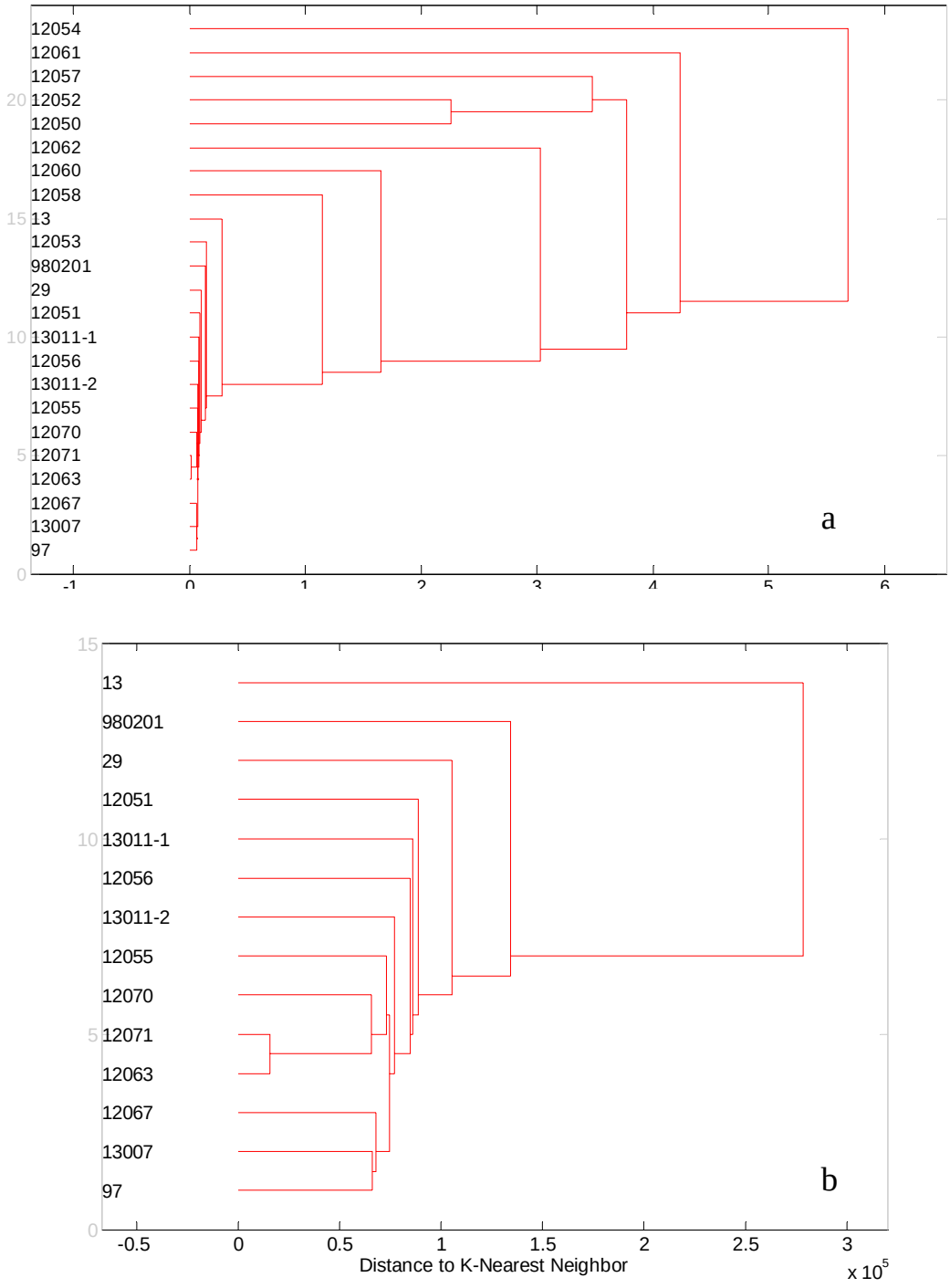

Figure 8: KNN dendogram of the unfolded LC-MS intensity matrices obtained from fake artesunate tablets. For a given pair of samples a small difference in their x-axis values denotes a high degree of similarity.

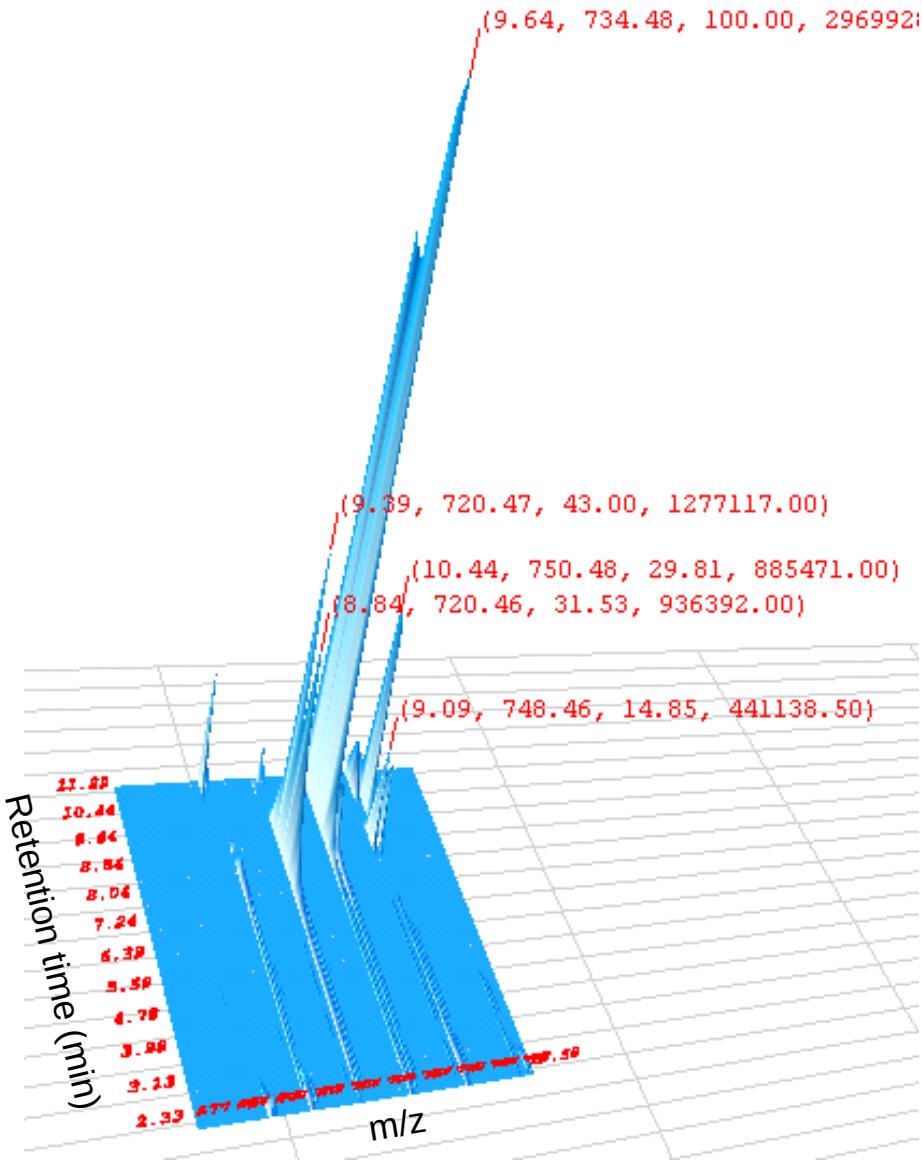

Figure 9: Three dimensional representation of the LC-MS intensity matrix for fake artesunate sample 12052 showing a detail of the region containing different. Peak labels describe retention time (min), m/z, relative intensity, and absolute intensity respectively. Intense signals are observed for the following erythromycin components: C at m/z = 720.5, A at m/z = 734.5, E at m/z = 748.5 and F at m/z = 750.5. The signals for anhydroerythromycin A at m/z = 716 m/z, and erythromycin B at m/z = 718 were not labeled for clarity. A threshold of 3% relative intensity was used to filter out background noise.

amount of erythromycin A was not the only variable determining the clustering of the samples. The different patterns of detected erythromycins seem to also influence the grouping into different sub-clusters. Table 3 lists the relative percent of other erythromycins in these samples expressed as % area.

Table 3: Erythromycin content in selected fake artesunate tablets. Absolute quantification was carried out only for erythromycin A. The approximate relative concentrations of other types of erythromycins are listed as the percent chromatographic peak area relative to the sum of the areas of all erythromycin-related compounds.

Sample	Erythro A Content (mg/g tablet)	Erythro A (% Area)	Erythro B (% Area)	Erythro C (% Area)	Erythro E (% Area)	Erythro F (% Area)	Anhydro-erythro A (% Area)
12054	27 ± 4	44.2	3.9	2.4	2.7	2.4	44.5
12061	191 ± 7	46.5	8.5	35.8	3.9	0	5.3
12057	58 ± 1	47.0	5.0	9.6	3.1	22.6	12.6
12052	57 ± 5	57.4	2.9	2.5	8.5	17.1	11.6
12050	50 ± 1	54.1	0.5	17.2	3.9	22.8	1.5
12062	20 ± 5	80.6	0.8	11.1	4.5	0	3.0
12060	<1	89.6	1.6	3.2	1.6	3.5	0.5
12053	<1	100	0	0	0	0	0

Some interesting observations can be derived if the sample clustering in the KNN dendrogram is examined together with the erythromycin A content, the pattern of erythromycins, the geographical origin and the type of fake hologram present in the packaging. For example, samples 12054 and 12061 showed the same type of rainbow foil

sticker (Type 5) and they were collected in different (but nearby) cities (Pakse and Salavan, Laos). These samples were placed in separate branches in adjacent positions at the top of the dendogram, indicating that although they may be related; there are significant differences between them. Both samples contained erythromycin A, but in different amounts (27 and 191 mg/g respectively), and different proportions of erythromycin C and anhydroerythomycin A (a hydrolysis product of erythromycin A), which explains the different placement in the dendogram. These samples both also contain $CaCO_3$ indicated via Raman spectroscopy analysis. Although one can only speculate at this point, these observations might indicate that these two samples stem from separate batches that originated in a common production source at early stages of the counterfeiting operation, where the sophistication of the fake holograms was still low.

Samples 12057, 12052 and 12050 are clustered as a sub-family of counterfeits which were all obtained in Pakse (Laos) and present similar rainbow foil stickers in their packaging (Types 8 and 12). These samples are different than samples 12054 and 12061, in that they all contain approximately 50 mg/g erythromycin A; however, they are the same in that they all contain $CaCO_3$. Samples 12052 and 12050 are further clustered into another subgroup, not far from sample 12057 due to their higher relative percentage of erythromycin A.

Samples 12062 and 12060 were both collected in Salavan (Laos) and presented similar rainbow foil stickers (Type 12 and 8). Their erythromycin fingerprint is similar (between 80 and 90% or erythromycin A) but they differ in their absolute erythromycin content. However, they are similar in that they both contain paracetamol. Sample 12058 (also presenting a Type 8 fake hologram) from Pakse, (Laos) does not contain erythromycin, and seems to be a class of its own, serving as a "boundary" between the Laos samples containing erythromycins with rainbow foil stickers and the remaining samples, all of them without erythromycins and presenting more elaborate packaging. Sample 12058 contained the signature for starch, and two medium intensity peaks separated by 304 mass units, previously not found in any other samples.

The analysis of the similarities among samples without erythromycins (13 to 97) reveals a few more interesting trends (Figure 8b). Sample 13, collected in Myanmar seems to be a class on its own, with no fake holograms or stickers present in the packaging. This sample, collected in Myitkyina (Myanmar) is the most isolated, from the rest of the samples from a geographical point of view. According to Raman, this sample also contains a starch compund. Sample 980201, collected in Ho Chi Minh City, presented no fake holograms and a very simple fingerprint which partially resembled the fingerprint from a second Vietnam sample, 29, presenting a Type 2 rainbow foil sticker. These two samples were found to

contain mostly $CaCO_3$ and might have been produced by the same manufacturing source, which added a fake rainbow foil sticker to its "product" in response to increased safety measures put in practice by the genuine manufacturers.

Very interestingly, samples with fake holograms Type 3 and 4 are grouped together, and were all collected either in Laos or neighboring Cambodia. Samples 12071 and 12063 seem to be almost identical from the chemical point of view, with matching fingerprints, and placed together in the dendogram. Their packaging contained Type 3 holograms in both cases, but were collected in different and fairly distant cities (one in northern Laos and one in southern Laos), a clear sign of a common production or distribution source. Both samples were found to contain starch and a fairly concentrated component presenting mass peaks at 438.3 u and 493.3 u, which could not be positively identified. Sample 12070, also collected in northern Laos, was chemically similar to 12071 and 12063, but presented the most sophisticated type of hologram (type 4), pointing that this sample might belong to a more recent batch. Samples 12051, 12055, 12056 and 13011 were collected in Pakse (Laos) and in the town of Anlong Veng in Cambodia (150 miles away) and appear to all be chemically related. All but 13011 contain a starch component. Sample 12056 presented a realistic Type 4 fake hologram, similar to the one found in sample 12070. The degree of similarity between samples with Type 3

and Type 4 fake holograms was much higher, if compared with the different samples containing erythromycins.

CHAPTER 5

CONCLUSIONS

This preliminary survey using LC-MS confirms the large prevalence of fake artesunate tablets with no detectable amount of active ingredient and reveals the presence of samples which contain subtherapeutic levels of artesunate. One of the most severe findings is that several "wrong" active ingredients were detected in the fakes. Multivariate clustering of the LC-MS chemical fingerprints allowed an in-depth investigation of the similarities between the samples for which it was observed that a correlation between sample origin, chemical composition and packaging exists, thus indicating that these "fakes" are the product of an organized international operation which has been flooding the market with fake artesunate over a period of several years.

CHAPTER 6

RECOMMENDATIONS

Clearly, the analysis of more samples by the approach presented here or a similar one would be beneficial. The main limitation of the present LC-MS methodology is its low sample throughput. For this reason, it is necessary for the development of an additional analytical method. Recently, two innovative MS-based high-throughput methods for the analysis of real samples, including pharmaceuticals, in open air have been reported. One of these described by Cooks et al. is DESI (Desorption Electrospray Ionization), which will increase the number of samples that can be analyzed in a time period of seconds or less.[44] Later, Cody et al. reported an atmospheric-pressure Penning ionization technique marketed under the name of DART® (Direct Analysis in Real Time).[30]It is expected that a DESI-based method will also be able to generate meaningful chemical fingerprints suitable to be examined via multivariate techniques.

It is also necessary to analyze a second sample set containing more than one hundred fake artesunate samples, to produce more densely populated clusters, which could lead to a better understanding of this complex issue and to eliminating this serious threat to public health.

APPENDIX A

SUPPORTING INFORMATION

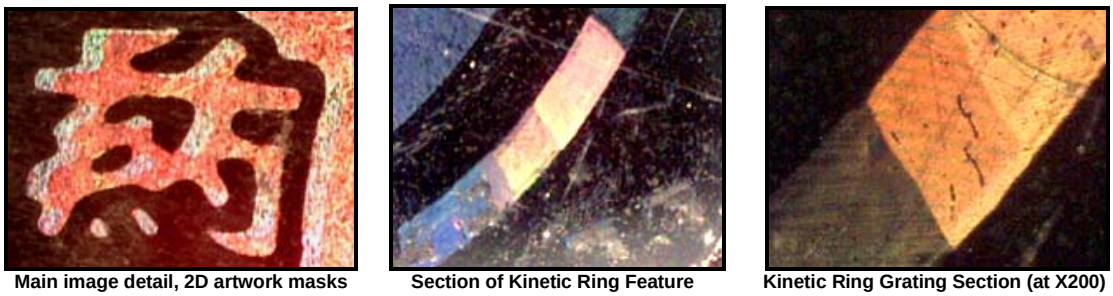

Main image detail, 2D artwork masks | Section of Kinetic Ring Feature | Kinetic Ring Grating Section (at X200)

Figure S-1: Detail of hologram from genuine artesunate tablets from Guilin Pharmaceutical.

The central image is made in the "2D-3D" style (generated from flat graphic line artwork) but with some variations from the traditional 2D-3D method. The image is only "2D" on the surface level, with no depth in the image. At 60x magnification the areas of grating section that have been exposed around the ring can be seen. At 200x magnification these sections can be seen to be doubly exposed in some areas. This is a very distinctive style, different from holograms used in North America and Europe

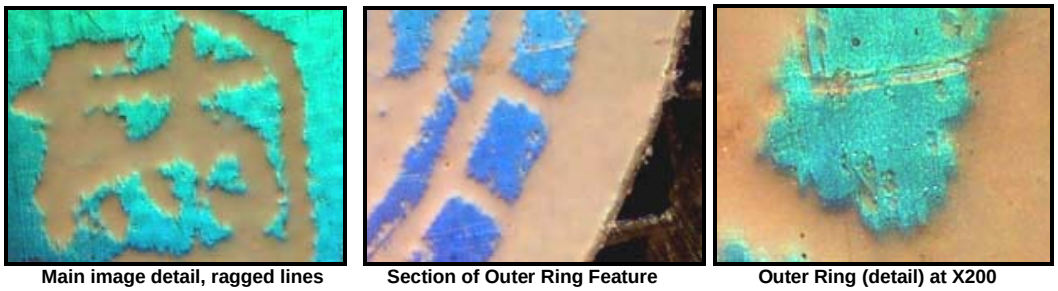

Main image detail, ragged lines | Section of Outer Ring Feature | Outer Ring (detail) at X200

Figure S-2: Detail of first generation (Type 2) fake hologram from fake artesunate tablets.

The fake 'hologram' affixed to Type 2 counterfeit artesunate is made from diffractive "rainbow" foil. Rainbow foil is usually over-printed with ink, or hot-stamped, to create an image that simulates a true hologram. The rainbow foil has been deep etched so as to remove selected areas of the surface and form an image.

Main image (detail) Chinese characters | Section of Outer Ring Feature | Outer Ring (detail) at X200

Figure S-3: Detail of second generation (Type 3) fake hologram from fake artesunate tablets.

The fake hologram attached to Type 3 counterfeit 'artesunate' is a simple 2D origination where the image is comprised of two exposures of diffractive color, one of which is much brighter than the other. The main exposure lights up the mountains and 50% of the sections in the outer ring of the image. This ring feature is not kinetic as in the genuine hologram and appears as a dashed line.

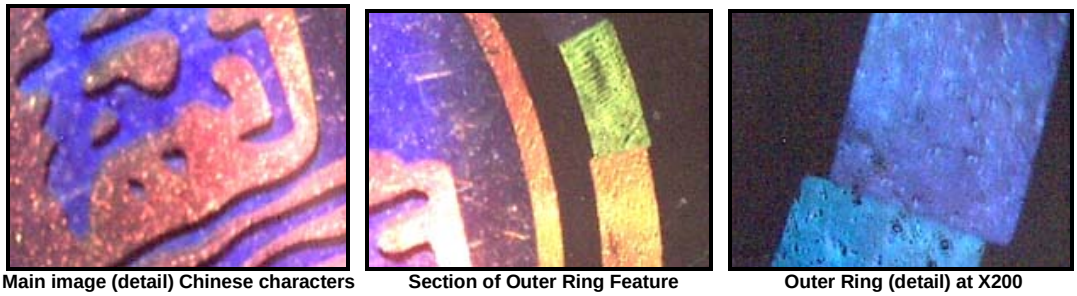

Main image (detail) Chinese characters | Section of Outer Ring Feature | Outer Ring (detail) at X200

Figure S-4: Detail of third generation (Type 4) fake hologram from fake artesunate tablets.

The fake holograms on the Type 4 'artesunate' counterfeits are very similar in appearance to the genuine hologram, despite using different techniques. The central image is a bright, clean, 2D image in two contrasting colors. Unlike the genuine hologram, both diffractive colors are made using the McGrew method[45] for making rainbow colors, (with diffused object beams, rather than un-diffused gratings) and thus have higher brightness than the genuine hologram. As in the genuine hologram, the kinetic feature of the outer ring is not composed of dots made by a dot-matrix machine, but it is formed of sections in three different diffractive colors (two of which are the same colors as the main image). These colors are repeated to provide an apparent animation when the hologram is tilted vertically, rather than right-to-left as in the genuine hologram.

REFERENCES

(1) *Fact Sheet N 275, World Health Organization* **2003**.

(2) O'Brien, K. L.; Selanikio, J. D.; Hecdivert, C.; Placide, M. F.; Louis, M.; Barr, D. B.; Barr, J. R.; Hospedales, C. J.; Lewis, M. J.; Schwartz, B.; Philen, R. M.; St Victor, S.; Espindola, J.; Needham, L. L.; Denerville, K. *Journal of the American Medical Association* **1998**, *279*, 1175-1180.

(3) Anonymous *Morbidity and Mortality Weekly Report* **1996**, *45*, 649-650.

(4) Hanif, M.; Mobarak, M. R.; Ronan, A.; Rahman, D.; Donovan, J. J.; Bennish, M. L. *British Medical Journal* **1995**, *311*, 88-91.

(5) Fackler, M. *San Francisco Examiner* **2002**.

(6) Wolff, J. C.; Thomson, L. A.; Eckers, C. *Rapid Communications in Mass Spectrometry* **2003**, *17*, 215-221.

(7) Newton, P. N.; White, N. J.; Rozendaal, J. A.; Green, M. D. *British Medical Journal* **2002**, *324*, 800-801.

(8) Goodman, P. S. In *International Herald Tribune*: Paris, 2002, pp 4.

(9) van Agtmael, M. A.; Eggelte, T. A.; van Boxtel, C. J. *Trends in Pharmacological Science* **1999**, *20*, 199-205.

(10) Daviss, B. *The Scientist* **2005**, *19*, 42-43.

(11) Wongsrichanalai, C.; Pickard, A. L.; Wernsdorfer, W. H.; Meshnick, S. R. *Lancet Infectious Diseases* **2002**, *2*, 209-218.

(12) Menard, R. *Nature (UK)* **2005**, *433*, 113-114.

(13) Wernsdorfer, W. H. *Acta Tropica* **1994**, *56*, 143-156.

(14) Kondrashin, A. V.; Rooney, W. *Southeast Asian Journal of Tropical Medicine and Public Health* **1992**, *23 Suppl 4*, 13-22.

(15) Aldhous, P. *Nature* **2005**, *434*, 132-136.

(16) Aldhous, P.; Akunyili, D. *Nature* **2005**, *434*, 134.

(17) Newton, P.; Proux, S.; Green, M.; Smithuis, F.; Rozendaal, J.; Prakongpan, S.; Chotivanich, K.; Mayxay, M.; Looareesuwan, S.; Farrar, J.; Nosten, F.; White, N. J. *The Lancet* **2001**, *357*, 1948-1950.

(18) Rozendall, J. *Bull Mekong Malaria Forum* **2000**, *7*, 62-68.

(19) Dondorp, A. M.; Newton, P. N.; Mayxay, M.; Van Damme, W.; Smithuis, F. M.; Yeung, S.; Petit, A.; Lynam, A. J.; Johnson, A.; Hien, T. T.; McGready, R.; Farrar, J. J.; Looareesuwan, S.; Day, N. P. J.; Green, M. D.; White, N. J. *Tropical Medicine and International Health* **2004**, *9*, 1241-1246.

(20) Deisingh, A. K. *Analyst* **2005**, *130*, 271-279.

(21) Vankeirsbilck, T.; Vercauteren, A.; Baeyens, W.; Van der Weken, G.; Verpoort, F.; Vergote, G.; Remon, J. P. *Trends in Analytical Chemistry* **2002**, *21*, 869-877.

(22) Abrahamsson, C.; Johansson, J.; Sparen, A.; Lindgren, F. *Chemometrics and Intelligent Laboratory Systems* **2003**, *69*, 3-12.

(23) Habib, I.; Kamel, M. *Talanta* **2003**, *60*, 185-190.

(24) Abrahamsson, C.; Johansson, J.; Andersson-Engels, S.; Svanberg, S.; Folestad, S. *Analytical Chemistry* **2005**, *77*, 1055-1059.

(25) Pachaly, P.; Schick, W. *Pharmazeutische Industrie* **1993**, *55*, 259-267.

(26) Phillips, G. *The Pharmaceutical Journal* **2003**, *271*, 465.

(27) Green, M. D.; Newton, P.; Fernandez, F. M.; Wirtz, R.; Nettey, H., London 2003; SMI Publishing.

(28) Green, M.; Mount, D. L.; Wirtz, R. A.; White, N. J. *Journal of Pharmaceutical and Biomedical Analysis.* **2000**, *24*, 65-70.

(29) Green, M.; Mount, D. L.; Wirtz, R. A. *Tropical Medicine and International Health* **2001**, *6*, 980-982.

(30) Cockburn, R.; Newton, P. N.; Agyarko, E. K.; Akunyili, D.; White, N. J. *Public Library of Science* **2005**, *2*, 100-106.

(31) Newton, P. N.; Dondorp, A.; Green, M.; Mayxay, M.; White, N. J. *Lancet* **2003**, *362*, 169-169.

(32) Drasar, P.; Moravcova, J. *Journal of Chromatography B* **2004**, *812*, 3-21.

(33) Massart, D. L.; Vandeginste, B. G. M.; Buydens, L. M. C.; De Jong, S.; Lewi, P. J.; Smeyers-Verbeke, J. *Handbook of Chemometrics and Qualimetrics*; Elsevier: Amsterdam, 1997.

(34) Antignac, J.; Le Bizec, B.; Monteau, F.; Poulain, F.; Andre, F. *Rapid Communications in Mass Spectrometry* **2000**, *14*, 33-39.

(35) Ortelli, D.; Rudaz, S.; Cognard, E.; Veuthey, J. *Chromatographia* **2000**, *52*, 445-450.

(36) Naik, H.; Murry, D.; Kirsch, L.; Fleckenstein, L. *Journal of Chromatography B* **2005**, *816*, 233-242.

(37) Hartl, D. L. *Nature Reviews Microbiology* **2004**, *2*, 15-22.

(38) de Veij, M.; Vandenabeele, P.; Hall, K. A.; Fernandez, F. M.; Green, M. D.; White, N. J.; Dondorp, A. M.; Newton, P. N.; Moens, L. *Analytical Chimica Acta* **submitted**.

(39) Rozendaal, J. *Lancet* **2001**, *357*, 890-890.

(40) Gates, P.; Kearney, G.; Jones, R.; Leadlay, P.; Staunton, J. *Rapid Communications in Mass Spectrometry* **1999**, *13*, 242-246.

(41) Newton, P.; Wellcome Trust SE Asian Tropical Medicine Research Units, 2005, pp 4.

(42) Allen Jr., L. V.; Popovich, N. G.; Ansel, H. C.; Allen, L. V. *Ansel's Pharmaceutical Dosage Forms and Drug Delivery Systems*, 8th ed.; Lippincott Williams & Wilkins: Philadelphia, 2004.

(43) Wardrop, J.; Ficker, D.; Franklin, S.; Gorski, R. *Journal of Pharmaceutical Sciences* **2000**, *89*, 1097-1105.

(44) Takats, Z.; Wiseman, J. M.; Gologan, B.; Cooks, R. G. *Science* **2004**, *306*, 471-473.

(45) McGrew, S. P. *Diffractive Color and Texture Effects for the Graphic Arts, Patent WO 82/01595*.